Nineteenth Australasian Wind Engineering Society Workshop, April 4-6, 2018, Torquay, Victoria

Reproducing AS/NZS terrain-type wind profiles in a short-fetch wind tunnel

Kevin[1], Jimmy Philip, Jason Monty and Joseph Klewicki

Dept. of Mechanical Engineering, University of Melbourne, Victoria 3010, Australia
[1]kevin.kevin@unimelb.edu.au

ABSTRACT

The model-testing wind tunnel at the University of Melbourne is adapted to produce AS/NZS terrain-type wind profiles. The eventual purpose of this effort is to develop turbulence and wind shear predictions around single or staggered buildings. When the usual strategies of generating Australian wind profiles, such as the use of rectangular blocks of various sizes, were employed, the turbulence levels were always too high. The main issue was the limited fetch of our test section. Here we develop a simple method to generate the required wind profiles using off-the-shelf tripping devices consisting of a row of spires, a square bar and a short synthetic grass patch. Step-by-step procedures to reproduce terrain category IV flow (urban-type area) are summarised. Here we systematically observe how the wind profiles change as the tripping configuration is altered. Overall, the merit of the present study is to determine the role of each tripping device as a means to better control the shape of the mean and turbulence intensity profiles. The essential ingredient involves the proper manipulation of the internal shear layers that are triggered by each tripping device.

1. Introduction

Understanding the interaction between turbulent flows and engineering/environmental structures is relevant to numerous applications. The endless combinations of building shape, orientation and arrangement (for example), coupled with the diverse wind conditions and limited resources, often makes direct quantification of such interactions nearly impossible. This limitation necessitates the development of simplified models and guidelines. Scaled wind-tunnel studies are particularly suitable for these purposes, especially when analytical solution becomes too complex to estimate wind loading and structural responses [Mendis (2007)]. Laboratory measurements have the advantage of being performed in a more controlled condition (compared to the field experiments), and the flow can be sampled longer to obtain a more reliable statistics.

The initial challenge, however, is certainly being able to simulate wind inputs that mimic the appropriate terrain/surface conditions, such as desert, grassland (airfield), suburban, or even the `rougher' city centres. In the Australian wind code AS1170.2, the above examples are referred to terrain category (hereafter will be referred to as TC) 1 to 4, respectively. It is important to note that it is only possible to reproduce the inner-most part of the atmospheric surface layer, and the main focus should be within the `roughness sublayer' (i.e., the flow region that is directly affected by surface topography). The wind profiles are typically simulated by overthickenning the boundary layer in the wind tunnel, using tripping devices such as spires, wedges, and distributed roughness elements [e.g. Counihan (1969), Irwin (1981), Sargison (2004), Talluru (2017)]. Attempts in utilising these common tripping configurations in our wind tunnel produced turbulence intensities (TI) that were higher than desired/expected. This most likely stems from the short test section, which prevents sufficient decay of the turbulence generated by the tripping devices.

The aim of the present study is therefore to systematically develop a simple tripping configuration, that can reproduce Australian wind codes, particularly terrain category 4, and in a short fetch wind tunnel.

2. Experiments

The $1{:}400$ ($z{:}z_{eq}$) scaled experiments are conducted in a wind-tunnel facility at the University of Melbourne. The 6-meter long working section of this wind tunnel has a prismatic cross-sectional area with dimensions illustrated in figure 1. The side walls of the test section are slotted, making it ideal for reducing the blockage effects [Smits and Baskaran (1980)]. This model-testing facility has recently been used to perform wake investigations of high cadence cycling at full scale [Chan (2017)]. To simulate the atmospheric boundary layer for the present study, a flat plate with an elliptical leading edge is mounted on the lower side of the working section. This configuration is illustrated in figure 1(a, c). Here the coordinate system x, y and z represent the windward, lateral and vertical directions respectively. A two-axis Velmex traversing system is mounted on the upper side of the test section, allowing both computer-controlled x and z movement. The velocity sensor used is a multi-hole pressure probe (Cobra Probe by Turbulent Flow Instrumentation), that has a frequency response up to 2 kHz. Although we also obtain both vertical (w) and lateral (v) turbulence signals, here we will focus on the streamwise/longitudinal velocity component (u). Sixteen data points are recorded in each vertical profile, taken at the centre of the test section (red dots in figure 1a). The sampling time for each position is 180 seconds at 2 kHz rate. Most of the velocity measurements are acquired at a flow development length of 4.8 m, unless otherwise stated. The datasets presented here are taken at a nominal free-stream velocity of U = 11.5 m/s, and changing this value by ± 5 m/s does not noticeably affect the normalised result (see figure 2). Also note that, here we only simulate the inner-most part of the surface layer, hence the highest measurement point is at $z = 300$ mm (or equivalent to $z_{eq} = 120$ m), with the reference height taken at 250 mm (or $z_{eq} = 100$ m) height. This limitation is partly due to the traverse and probe configurations.

To artificially thicken the boundary layer and to induce larger-size turbulence, a row of trapezoidal spires is mounted near the leading edge. Figure 1(b) illustrates how the spires are

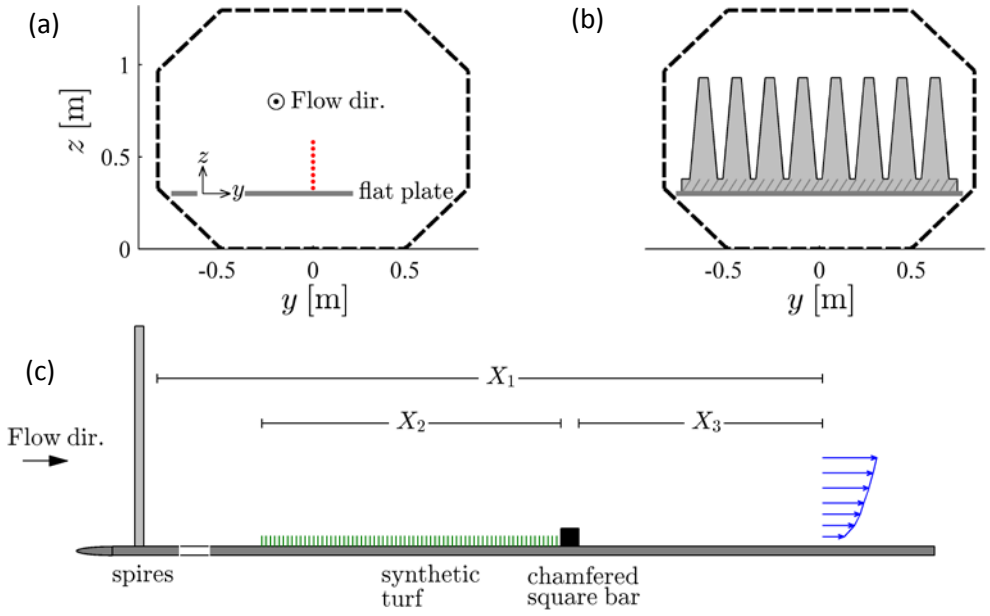

Fig. 1. (a, b) Cross sectional area of the model testing wind tunnel, illustrating the slotted side walls and one of the spires setup. (c) Flow tripping arrangement to generate the AS/NZ wind profiles. X_1, X_2 and X_3 indicate the distance/extent of the measurement station and tripping devices.

configured in the test section, and figure 1(c) pictures the side view. The base (hatched region in figure 1b) of the spires is 80 mm high, and the trapezoidal elements are 0.5 m tall. The lateral spacing of each spire is 180 mm, giving spacing/height ratio of approximately 0.3. The relatively small spacing (typically for ratio of < 0.5) prevents the lateral flow variation in the wind tunnel [Counihan (1969); Irwin (1981)]. Additionally, the development length of more than 8 times the spires height, as well as the addition of the subsequent tripping devices enhances the uniformity of the turbulence closer to the surface. Here the streamwise distance from the spires to the measurement station is denoted as X_1. To further increase the momentum deficit near the surface, a synthetic grass patch (20 mm grass height) and a chamfered-edged squared bar (with cross-section of 40×40 mm) is added. Here the streamwise length of the grass patch, and the distance from the square bar to the measurement station are referred to as X_2 and X_3 respectively.

3. Results for terrain category 4 and the role of each tripping device

Figure 2 shows the resulting wind profiles for terrain category (TC) 4, generated using the tripping configuration specified in the previous section. In this case, X_1, X_2 and X_3 are $4.8, 1.0$ and 0.45 m, respectively. The shape of the mean velocity deficit agrees well with the site wind speed $U_{site}(z)$, prescribed by Standards Australia (2011),

$$U_{site} = U_R \, M_{category} \;\; (M_d \, M_s \, M_t)$$

plotted in solid line. Here $U_R(z)$ is the regional wind profile, where we use region category `A' defined by Standards Australia (2011) for non-cyclonic wind speed. $M_{category}(z)$ is terrain-category multiplier, which in this case we choose to simulate an urban area or TC4. Since M_d (wind direction), M_s (shielding type) and M_t (topographic-type) multipliers are not functions of elevation z, their effects will fall under the velocity normalization. In figure 2(b), we also superimpose reference TI profile tabulated in Standards Australia (2011). Good agreement is observed between the experimental result and this reference profile. The slight overestimation of TI for $z > 150$ mm is addressed in a later discussion. As indicated by the red and blue-coloured symbols, altering the inlet velocity by ± 5 m/s barely alters the normalized velocity results.

The normalized turbulence-spectral-densities for three elevations are shown in figure 3(a), where the results are compared against the spectral model of Harris (1990), which is used by Standards Australia (2011). The spectral behaviour appears to follow the model for all the comparisons. Additionally, all spectral distributions appear similar across different heights. This behavior is consistent with observation by Talluru *et al.* (2017) who further observed this similarity across terrain categories (i.e. roughness level). In figure 3(b) we further plot the energy spectra against the frequency, where a clear -5/3 gradient is apparent in the log-log plot. The slight deviation

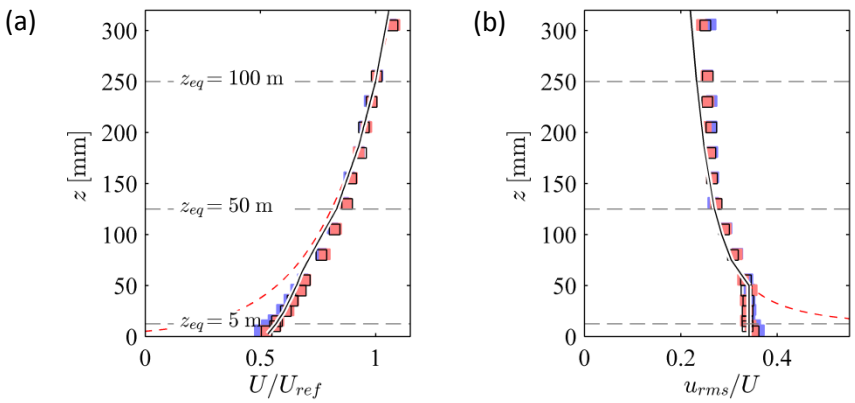

Fig. 2. Comparison between scaled (a) mean and (b) turbulent intensity profiles of TC4 at $U_\infty = 11.5$ m/s, between: experimental data (points), profile from AS/NZS 1170.2:2011 (black line) and Deaves & Harris model (red dotted line). Black, blue and red points: tests at 11.5 m/s and at lower/higher inlet velocities of $\pm$ 5 m/s respectively.

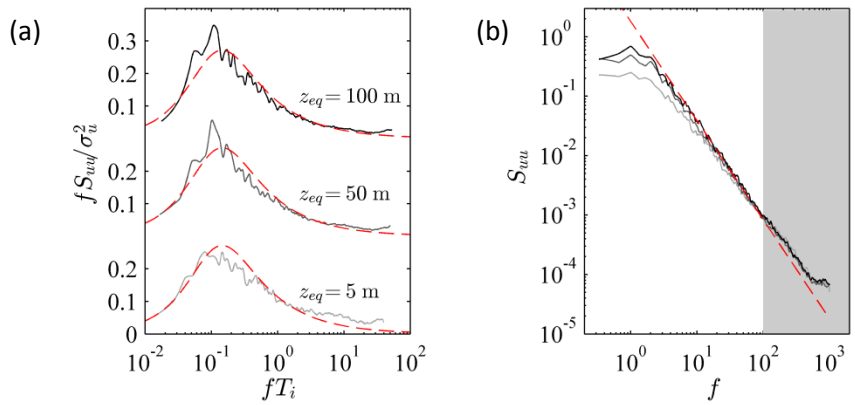

Fig. 3. Spectral density at three elevations indicated at figure 2. (a) In a normalised form. Red dashed lines: Spectral model of Harris (1990). (b) The corresponding spectra against frequency. Red dashed line: $-5/3$ gradient. Shaded region: frequency range affected by experimental noise.

from this behavior at frequency of > 100 Hz is due to the contamination of experimental noise. Overall, both first and second order velocity statistics, as well as the turbulence spectra are shown to adhere to the Standards Australia (2011) for TC4 wind profile.

Now we shall present how these velocity profiles are constructed. The top and bottom panels in figure 4 display the corresponding pair of mean and TI profiles. Figure 4(a, e) shows the baseline profiles, i.e. a flat-plate boundary layer. The natural boundary layer thickness is about 90 mm, and the turbulence level above the layer (in the free-stream flow) is low ($\sim 0.5\%$). Clearly these profiles do not represent TC4 wind behavior, displayed by the solid line. After the spires are placed (figure b, f), we gain some portion of the mean flow deficit as well as the bulk TI. Note that there is a slight overshoot in the TI (red box in figure 4f), that will be carried over to figure (g, h). As later discussed, this is due to the spires being too large (and dense) or the lack of streamwise development length. To further introduce momentum deficit and TI close to the surface, a square bar is mounted 0.45 m upstream the measurement station. The resulting profiles are shown in figure 4(c, g).

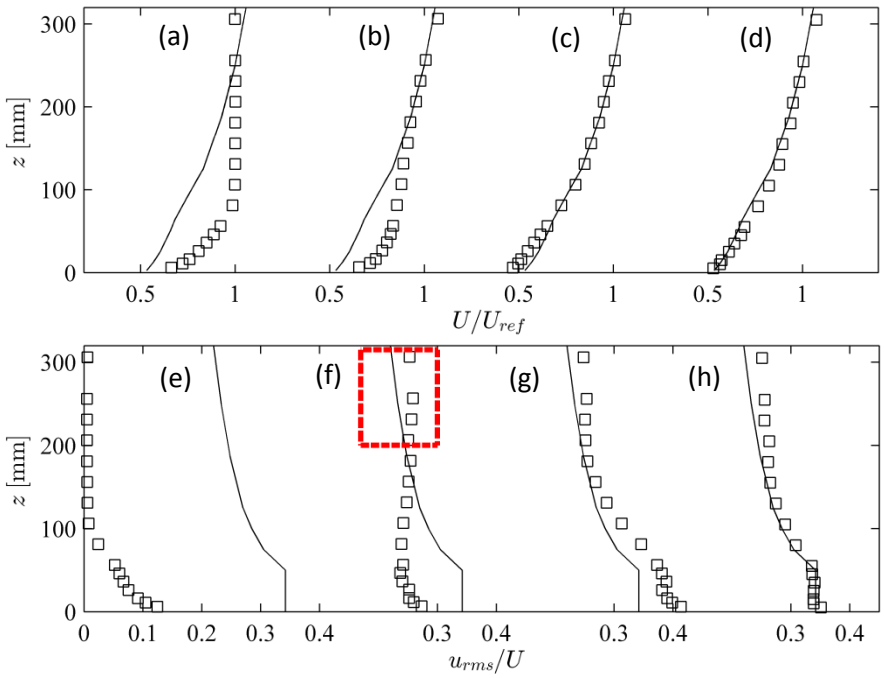

Fig. 4. The change in wind profile as tripping device is added. Top and bottom: mean and turbulence intensity. (a, e) Flat plate boundary layer; (b, f) with spires only; (c, g) with spires and bar; (d, h) with spires, bar and grass. Solid lines: reference profiles from Standards Australia (2011).

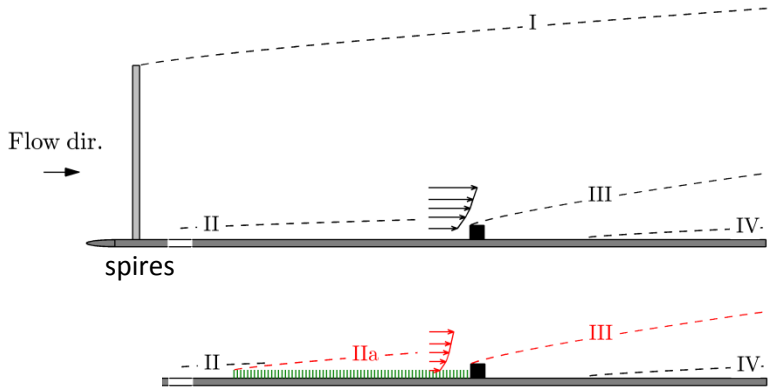

Fig. 5. Schematic of the internal and external boundary layers produced by the current tripping devices. Top/bottom: without/with grass. II, III and IV are internal shear layers formed by the trips.

Despite the good agreement between the mean flow and its reference profile, the TI values clearly exceed the intended magnitude. To counteract this effect, we placed a 1 m long grass (roughness) patch prior to the square bar. The resulting profiles are shown in figure 4(d, h), where both mean and TI follows the prescribed profiles by Standards Australia (2011). At first, placing a roughness patch over a smooth surface in order to reduce/control the overall turbulence output may seem counter intuitive. The key is to realise that the grass patch (despite generating its own turbulence) slows the overall mean flow that is approaching the square bar. This effect is better illustrated by figure 5, where the internal boundary layer labelled `IIa', which is the result of the smooth-grass transition, yields lower mean flow distribution close to the surface. Since the turbulence produced by the square bar is proportional to the incoming wind speed, the reduced velocity due to the grass patch reduces the TI. Though not shown here, halving the length of grass patch barely alters the result.

4. The effect of spires size and on generating lower terrain category

As previously mentioned, the spire geometry governs the bulk TI magnitude especially in the outer flow. In this instance, we attempt to reduce the overshoot in the TI (in the outer flow), that appears in figure 4(f-h). Here a new set of spires with the same height but slightly larger spacing of 230 mm (in contrast to 180 mm) is employed, and the result is compared in figure 6(a, b). It is clear that the overall TI more closely follows the standard profile, while the mean velocity is still in a good agreement. Note that in this case the measurement station is $X_1 = 3.8$ m downstream the spires, while the distance between the square-bar and the probe is $X_3 = 0.39$ m. The grass patch remains at 1 m fetch. In achieving these new results, we follow the step-by-step observation illustrated in figure 4. Additionally, we further assess whether wind profiles from other TCs, which require much lower turbulence intensity, can be generated using this tripping configuration. Figure 6(c) shows how the TI values at $z = 250$ mm (or $z_{eq} = 100$ m elevation), changes with measurement location X_1. The red symbol indicates the required turbulence level for TC3 at this elevation. This is the same value shown in figure 6(d) for the TC3 wind profile. A power law fit through the data in figure 6(c) indicates that $X_1 = 7.3$ m is required for the turbulence generated by this particular spire configuration to decay. This is not attainable, however, since this distance is longer than our test section. Therefore, we have to further reduce the size of the spires, and these tests are presently being conducted.

5. Conclusions

A series of experiments are conducted in an attempt to produce velocity profiles which adhere to AS/NZS wind code. Due to the limited test-section length, the usual flow-tripping strategy, such as the use of roughness floor (or blocks), were not effective. As such, we developed a new set of tripping arrangements for shorter fetch wind-tunnels. Using off-the-shelf tripping devices, consisting of a row of spires, a square bar and a short synthetic grass patch, our results for flows over urban area, characterized by the mean velocity, turbulence r.m.s., and the spectral density agree well with

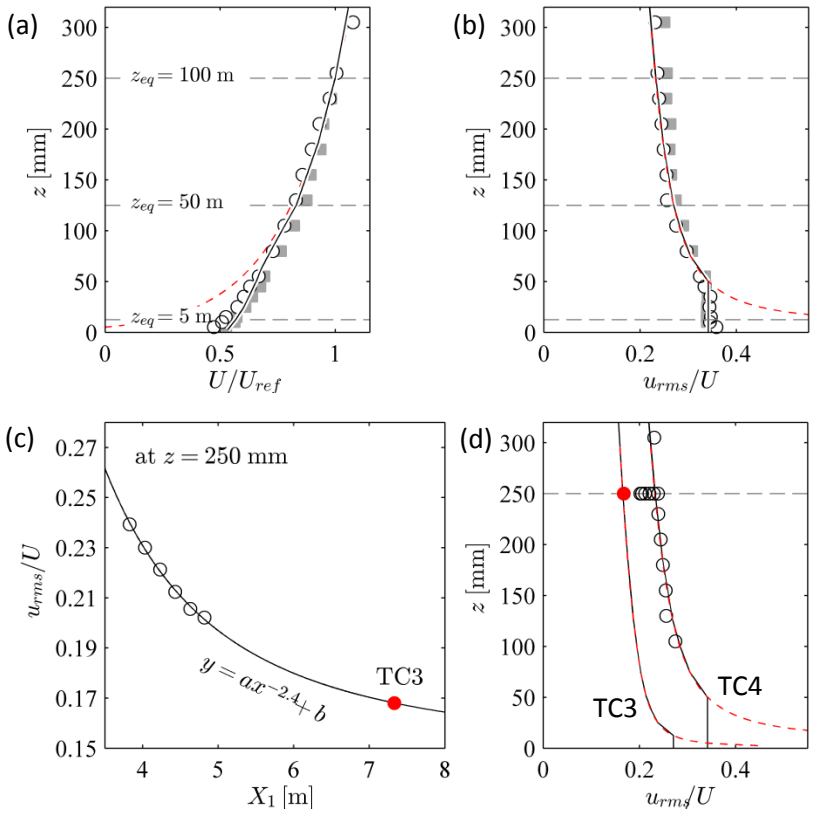

Fig. 6. Comparison between (a) mean and (b) turbulence intensity between the denser spires with 180 mm spacing (square) and the slightly sparser with 230 mm spacing (circle). (c) Turbulence intensity decay with distance from the 230 mm spacing spires at $z = 250$ mm. Red dot: the required turbulence level for TC3. (d) The change of TI at $z = 250$ mm with distance.

the standards. The step-by-step guideline is summarized by systematically observing how the wind profiles changes as the tripping configuration is altered. The key here is being able to incorporate multiple internal shear layers that are triggered by each device/surface used as trips.

References

Chan H. C., 2017. Wake drag structure of high cadence cycling. PhD thesis. The University of Melbourne.

Counihan J., 1969. An improved method of simulating an atmospheric boundary layer in a wind tunnel. *Atmospheric Environment.* 3(2):197–214

Harris R. I., 1990. Some further thoughts on the spectrum of gustiness in strong winds. *J. Wind Eng. Indus. Aero.* 33(3):461–477

Irwin H. P. A. H., 2010. The design of spires for wind simulation. *J. Wind Eng.* 7:361–366

Mendis P., Ngo T., Haritos N., Hira A., Samali B., Cheung J. 2007. Wind loading on tall buildings. *EJSE Special Issue: Loading on structures.* 3:41–54

Sargison J. E., Walker G. J., Bond V., Chevalier G. 2004. Experimental review of devices to artificially thicken wind tunnel boundary layers. *Proceedings of the Fifteenth Australasian Fluid Mechanics Conference*, Sydney, Australia, Dec 13-17, 2004.

Smits A. J., Baskaran V. 1980. Two-dimensional solid blockage in slotted wall wind tunnel. *Proceedings of the Seventh Australian Conference on Hydraulics and Fluid Mechanics*, Australia.

Standards Australia, (2011), "Structural design actions. Part 2 Wind actions", Australian/New Zealand Standard, AS/NZS 1170.2:2011.

Talluru K. M., Hernandez-Silva C., Chauhan K. A. 2017. Wind tunnel simulation of terrain categories specific to Australian wind code. *Proceedings of the Ninth Asia-Pacific Conference on Wind Engineering*, Auckland, New Zealand, Dec 3-7, 2017.